Energy transfer efficiency distributions in polymers in solution during folding and unfolding

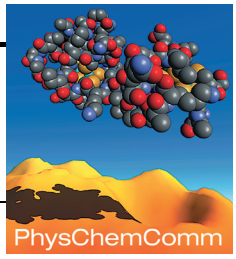

Paper

Goundla Srinivas and Biman Bagchi*

Solid State and Structural Chemistry Unit, Indian Institute of Science, Bangalore, India 560 012. E-mail: bbagchi@sscu.iisc.ernet.in

Received 18th January 2002, Accepted 14th February 2002
Published on the Web 26th February 2002

Distribution of fluorescence resonance energy transfer (FRET) efficiency between the two ends of a Lennard-Jones polymer chain both at equilibrium and during folding and unfolding has been calculated, for the first time, by Brownian dynamics simulations. The distribution of FRET efficiency becomes **bimodal** during folding of the extended state subsequent to a temperature quench, with the width of the distribution for the extended state broader than that for the folded state. The reverse process of unfolding subsequent to a upward temperature jump shows different characteristics. The distributions show significant viscosity dependence which can be tested against experiments.

1 Introduction

Dynamics of polymer folding and unfolding in solution is a problem of much current interest.[1–3] Although some aspects of polymer folding appears to be understood, detailed experimental study of the folding scenario (especially the initial part) is still not available. Given the complexity of the problem, the computer simulations could consider only relatively simple models, such as a necklace of Lennard-Jones or square-well beads. In addition to its own intrinsic interest, the collapse of polymers from poor solvents has served as a theoretical model of protein folding in the early stages.[4–8]

In a notable recent development, fluorescence resonance energy transfer (FRET) has been combined with single molecule spectroscopic (SMS) technique to provide a powerful novel approach to study the dynamics of folding. Deniz *et al.*,[9] reported studies of dynamics of protein folding by observing FRET in time domain from a *single* donor–acceptor (D–A) pair. In the measurement of Deniz *et al.*, the *subpopulations*[9–11] of the folded and denatured states of the protein chymotrypsin inhibitor 2 (CI2) were obtained as the concentration of the denaturant (guanidinium chloride) was varied. The most interesting result was that at the intermediate concentration of the denaturant, the distribution of Forster efficiency becomes *bimodal*. It was concluded that this bimodal distribution is the signature of the ''two state' nature of CI2 folding transition. We were curious to know whether such a bimodal distribution can be observed (a) for simple models like collapsing homopolymers and (b) whether it can originate from dynamics alone. To answer these questions, we have carried out extensive Brownian dynamics (BD) simulations of FRET in single macromolecules. We find, surprisingly, that even such a simple system shows a bimodal distribution in the excitation transfer efficiency, for chosen sets of parameter values. The double peak is similar to the ones observed in experiments.[9] The bimodal distribution is observed not only during folding but also at equilibrium near the θ temperature. The results obtained here should help in designing future experiments.

The usually assumed mechanism for FRET is the Forster energy transfer (FET).[12,13] The rate of this transfer depends on the separation (R) between the energy donor and the energy acceptor. This rate, $k(R)$, can be written as,[12]

$$k(R) = k_{\mathrm{rad}} \left(\frac{R_{\mathrm{F}}}{R} \right)^6 \tag{1}$$

where R_{F} is the Forster radius and k_{rad} is the radiative rate, which is typically in the range 10^8 to 10^9 s^{-1} for the commonly used chromophores. The rate of energy transfer becomes equal to K_{F} when $R = R_{\mathrm{F}}$. For a given D–A pair, R_{F} can be obtained by the usual method of overlap between the fluorescence and the absorption spectra of the D–A pair.[12] For commonly used chromophores, R_{F} is fairly large, often as large as 50 Å. This means that the rate is very large when the donor–acceptor pair is separated by a short distance. This may actually be a limitation of the Forster expression which is strictly valid when the separation between the D–A pair is much larger than their size. However, the above limitation shall have a minor effect in the present study which is qualitative in nature and aims at exploring the general aspects of the energy transfer efficiency distribution during folding.

In writing eqn. (1), the standard averaging over the orientations of the transition dipole moments has been carried out. In standard FRET experiments, the macromolecule is doped with a D–A pair in suitable locations along the chain.[13] Excitation transfer can be monitored by following the fluorescence either from the donor or the acceptor or from both. The time, τ_{rxn}, taken for the excitation transfer to occur depends strongly on the D–A separation R, as given by $k(R)$ in eqn. (1). For a polymer (or a protein) in solution, both at equilibrium and during folding/unfolding, R is not only a fluctuating, stochastic function of time, but also varies in a definite way. In such cases, the distribution of the energy transfer efficiency contains non-trivial and useful information. Note that simulating FRET in real proteins is an exceedingly difficult problem – it is not trivial even for a simple homopolymer – a problem that has eluded theoretical description even today.

We define the FRET efficiency (Φ_{F}) by the following relation,

$$\Phi_{\mathrm{F}} = \frac{k(R)}{k(R) + k_{\mathrm{rn}}}, \tag{2}$$

where k_{rn} is the radiative decay (other than Forster migration)

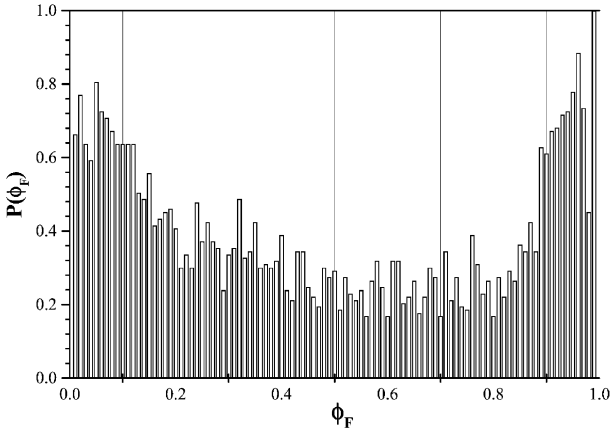

Fig. 1 The distribution of FRET efficiency ($P(\Phi_F)$), subsequent to a temperature quench (from $\varepsilon^* = 0.1$ to $\varepsilon^* = 0.8$), obtained from BD simulations is shown at $R_F = 7$, $\tilde{k}_{rad} = 10$ and $N = 80$. This demonstrates the emergence of bimodality in $P(\Phi_F)$. Here k_{rn} is fixed as 0.0001; the bimodality is present at other values also, but sharpness depends on the magnitude of the radiative rate.

of the donor–acceptor pair. We next define the FRET efficiency distribution $P(\Phi_F)$ by the following expression,

$$P(\Phi_F) = \frac{1}{N}\sum_{i=1}^{N} \delta(\Phi_F - \Phi_F(\tau_{rxn})). \quad (3)$$

The above equation is to be understood in the following fashion. After choosing a D–A pair at time $t = 0$, the pair is followed till the trajectory gets terminated due to the reaction.

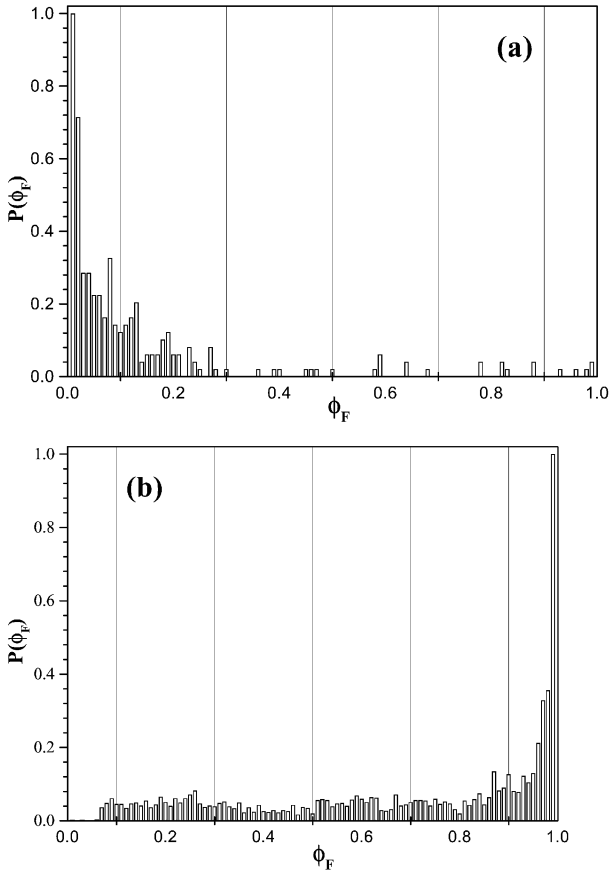

Fig. 2 The equilibrium FRET efficiency (Φ_F) distribution is shown for (a) $\varepsilon^* = 0.3$ and (b) $\varepsilon^* = 0.8$. $\tilde{k}_{rad} = 10$ and $R_F = 7$ while k_{rn} is fixed as 0.01.

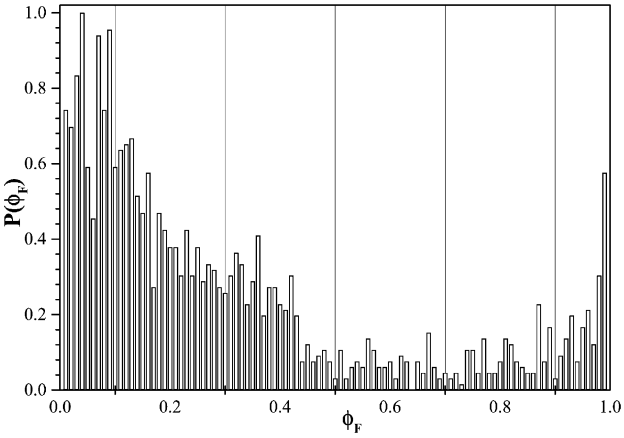

Fig. 3 The equilibrium FRET efficiency distribution ($P(\Phi_F)$) is shown for $\varepsilon^* = 0.5$, which is close to the θ temperature ($\varepsilon^*_\theta = 0.62$). $\tilde{k}_{rad}$, R_F and k_{rn} are same as in Fig. 2. This figure demonstrates the emergence of bimodality even at equilibrium.

We define this time by τ_{rxn}. At this time, the existing end-to-end distance (R) is used in eqn. (2) to calculate Φ_F. This was followed for N independent trajectories for pairs chosen from an equilibrium distribution. At the end we distribute the FRET efficiencies in to the bins of width 0.1. In this way, a continuous probability distribution ($P(\Phi_F)$) can be obtained from eqn. (3), by taking the $N \to \infty$ limit – in our case, we get a histogram (Fig. 1–4). Similarly, we can calculate the probability distribution of reaction times.[15]

In this paper, we present the calculations of the distribution of $P(\Phi_F)$ for Forster migration among polymer ends both at equilibrium and *during folding and unfolding*. In the next section we describe the model and the simulation details. In section III we present the results. We close the paper with a few conclusions in section IV.

2 Simulation details

2.1 The model

The model polymer chain is made of connected Lennard-Jones (LJ) beads. While this model homopolymer does not represent complex richness of a protein, it is known to show interesting folding kinetics.[2,3] The total potential energy can be written as,[2]

$$U = \sum_{i=2}^{N}\sum_{j=1}^{i-1} u_{LJ}(\boldsymbol{r}_{ij}) + \sum_{i=2}^{N} u_b(|\boldsymbol{r}_i - \boldsymbol{r}_{i-1}|) \quad (4)$$

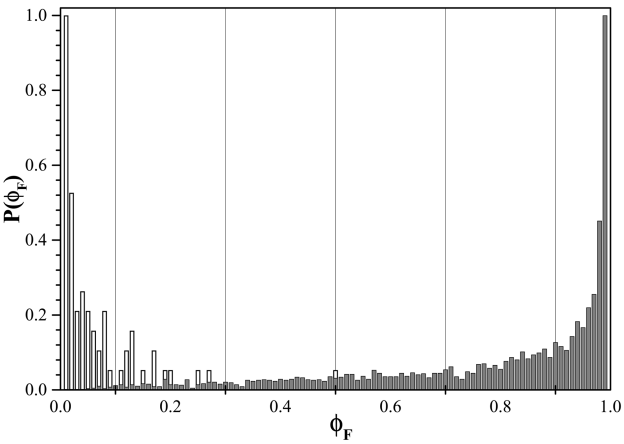

Fig. 4 FRET efficiency distribution ($P(\Phi_F)$), subsequent to quench (from $\varepsilon^* = 0.1$ to $\varepsilon^* = 0.8$) is shown for $\tilde{k}_{rad} = 1$ (open bars) and $\tilde{k}_{rad} = 10$ (filled bars). $R_F = 7$ and k_{rn} are same as in Fig. 2.

where N is the number of beads, $\boldsymbol{r}_i$ is the position of bead i, $r_{ij} = |\boldsymbol{r}_i - \boldsymbol{r}_j|$, $u_{\mathrm{LJ}}(r)$ is the LJ potential,

$$u_{\mathrm{LJ}}(r) = \varepsilon\left[\left(\frac{\sigma}{r}\right)^{12} - \left(\frac{\sigma}{r}\right)^{6}\right] \tag{5}$$

u_{b} is the bonding potential,

$$u_{\mathrm{b}} = \frac{3\kappa k_{\mathrm{B}}T}{2b^2}\sum\left(\left|\boldsymbol{r}_i - \boldsymbol{r}_j\right| - b\right)^2 \tag{6}$$

where σ and ε are the LJ collision-diameter and the well depth, respectively, $k_{\mathrm{B}}T$ is the thermal energy and κ represents the stiffness of the spring. Here, we use $\kappa = 9$, $N = 80$, and $b = \sigma$. For convenience, we define $\varepsilon^* = \varepsilon/k_{\mathrm{B}}T$. The unit of time, τ, is b^2/D_0. Thus, $\tilde{k}_{\mathrm{rad}}$ ($\equiv k_{\mathrm{rad}}b^2/D_0$) is also dimensionless. In this study we have chosen $\tilde{k}_{\mathrm{rad}} = 1$ and 10. This choice of $\tilde{k}_{\mathrm{rad}}$ corresponds to the experimentally observed k_{rad} values, a bit biased towards higher values. For example, in a solvent with viscosity (η) equal to 1 cp, the radius of monomer molecules (R) equal to 4 Å, $\tilde{k}_{\mathrm{rad}} = 1$ corresponds to a k_{rad} of 0.76 ns^{-1} while $\tilde{k}_{\mathrm{rad}} = 10$ corresponds to that of 7.6 ns.[14] R is scaled by b, the bead diameter, as usual. In viscous solvents, the viscosity can be much higher, and the $\tilde{k}_{\mathrm{rad}}$ can be even larger than 10.

The time evaluation of the polymer chain is done according to the following equation of motion,

$$\boldsymbol{r}_j(t+\Delta t) = \boldsymbol{r}_j(t) + F_j(t)\Delta t + \Delta X^{\mathrm{G}}(t) \tag{7}$$

where $\boldsymbol{r}_j(t)$ is the position of jth bead at time t and the systematic force on j is denoted by $F_j(t)$. The random Brownian displacement, $\Delta X^{\mathrm{G}}(t)$, is taken from a Gaussian distribution with zero mean and $2\Delta t$ variance. The time step, Δt, is varied from 0.0001 τ to 0.0005 τ. The scheme of Noguchi and Yoshikawa[2] has been used to investigate the polymer folding. In this method, the equilibrium configuration obtained at $\varepsilon^* = 0.1$ is quenched by decreasing the temperature instantaneously to different values of ε^*, higher than 0.62 which is the θ temperature in this model. The time dependent total energy, the root mean square end-to-end distance (R^2) and the radius of gyration (R_{g}^2) were all monitored to follow the progress of folding. The results presented here are the average over 10,000 of such trajectories with different initial configuration. More details on the simulation scheme can be found elsewhere.[15] To simulate FRET , we have probed many combinations of R_{F} and $\tilde{k}_{\mathrm{rad}}$. We have selected $R_{\mathrm{F}} = 7$, which is near the maximum in $R^2P(R)$ (we denote it by R_0), where $P(R)$ is the end-to-end distribution. Another important parameter which affects FRET is $\tilde{k}_{\mathrm{rad}}$. Large $\tilde{k}_{\mathrm{rad}}$ values result in the higher efficiency of FRET. In this study we have mostly dealt with $\tilde{k}_{\mathrm{rad}} = 10$.

2.2 Time scales

FRET in polymers involves *several* different time scales. Two time scales, τ_{Ffold} and τ_{Fun}, are required to describe the average survival probability of FRET in the folded and unfolded states, respectively.[15] These two time scales are widely separated from each other, due to the sensitivity of survival time to the separation between the two ends. The third relevant time in this problem is τ_{qfold}, the time required for the polymer to fold subsequent to the quench. For FRET to be useful in the study of folding, this τ_{qfold} should be intermediate and well-separated from the other two times. Two additional time scales k_{rad}^{-1} and b^2/D_0 come from Forster energy transfer and Brownian dynamics, respectively. While k_{rad} is fixed, b^2/D_0 can be varied by changing viscosity (η).

3 Results and discussion

Results for the distribution *during* folding process (subsequent to the quench from $\varepsilon^* = 0.1$ to $\varepsilon^* = 0.8$) are shown in Fig. 1. In this figure the simulated probability distribution of FRET efficiency $P(\Phi_{\mathrm{F}})$ during folding is plotted at $R_{\mathrm{F}} = 7$ and $\tilde{k}_{\mathrm{rad}} = 10$. One sees a clear bimodal distribution in the FRET efficiency. The first peak at low efficiencies arises from the extended state while the one at high efficiencies arises from the folded configurations. Note also that the distribution for the extended state is broad while that from the collapsed state is narrow. This is expected on physical grounds and has been observed in experiments. This bimodality is found to depend critically on the value of k_{rn} which is a consequence of several competing time scales in the FRET.

Results presented in Fig. 1 can be better understood from Fig. 2 where we have plotted the *equilibrium* FRET efficiency distribution in the extended (unfolded) and the collapsed (folded) states, at $R_{\mathrm{F}} = 7$ and $\tilde{k}_{\mathrm{rad}} = 10$. It is observed that the time taken for FRET is much larger in the unfolded state (Fig. 2a), compared to that in the folded state (Fig. 2b). This is reflected in the (ensemble averaged) survival probability ($Sp(t)$) of D–A pair (not shown), which is extremely fast in the collapsed state and very slow in the extended state. The reason for the observed (nearly) exponential distribution for the unfolded state (Fig. 2a) lies in the choice of R_{F}. Since maximum probability for end-to-end distance (obtained by maximizing $R^2P(R)$) is at $R \approx 7.3$, for the given temperature and interaction strength. Thus, at $R_{\mathrm{F}} = 7$, there is significant population already at this distance. If we change R_{F} to small (like $R_{\mathrm{F}} = 1$) or large (like $R_{\mathrm{F}} = 10$) values, the exponential distribution will be replaced by a Gaussian type distribution. This sensitivity of the distribution to R_{F} can be exploited in experiments. The distribution of reaction efficiencies in the folded state (Fig. 2b), however, is *not* exponential. The initial fast fall in the probability is followed by a somewhat slower decay.

Both at high ($\varepsilon^* \approx 0.1$–$0.3$) and low temperatures ($\varepsilon^* \approx 0.8$–$0.9$) the equilibrium $P(\Phi_{\mathrm{F}})$ shows a single peak at lower and higher FRET efficiencies, respectively. However, at intermediate temperatures($\varepsilon^* \approx 0.5$–$0.6$), the equilibrium FRET efficiency distribution ($P(\Phi_{\mathrm{F}})$) again shows a bimodal distribution. This is shown in Fig. 3, where the equilibrium $P(\Phi_{\mathrm{F}})$ is plotted at $\varepsilon^* = 0.5$. The emergence of bimodality in $P(\Phi_{\mathrm{F}})$, even at equilibrium, is due to the closeness to the θ temperature ($\varepsilon_\theta^* = 0.62$). This indicates that a "two-state' model exists in this simple system of homopolymer chain, near the θ temperature.

The above observations seem to provide the following interpretation of the observed bimodality in Fig. 1. As the polymer collapses subsequent to the quench, the polymer passes through a succession of configurations. The initial configurations correspond to the extended state. The polymer passes through the intermediate state rather fast which shows the dearth of population at intermediate Φ_{F}, giving rise to the bimodality.

The effect of viscosity (η) can be studied by varying the dimensionless rate $\tilde{k}_{\mathrm{rad}}$, defined as $k_{\mathrm{rad}}b^2/D_0$. At constant k_{rad}, large values of $\tilde{k}_{\mathrm{rad}}$ represent solution of high viscosity and *vice versa*. In Fig. 4, $P(\Phi_{\mathrm{F}})$ is plotted against the FRET efficiency at two very different values of $\tilde{k}_{\mathrm{rad}}$. Open bars show the result for $\tilde{k}_{\mathrm{rad}} = 1$, while the filled bars represent that for the $\tilde{k}_{\mathrm{rad}} = 10$. Fig. 4 shows that viscosity can have a dramatic effect on FRET efficiency distribution.

During the unfolding (when the temperature is instantaneously raised to $\varepsilon^* = 0.1$ from $\varepsilon^* = 0.8$), $P(\Phi_{\mathrm{F}})$ shows a large peak at higher efficiencies which is accompanied by a tail (of smaller peaks) towards lower efficiencies. The probability distribution of reaction times (subsequent to a temperature quench) $P(\tau_{\mathrm{rxn}})$ also shows a bimodal distribution. We have found that one can efficiently study the dynamics of the initial stages of folding by placing the pair near the chain end where the nucleation of the collapse starts in nearly all the cases that we studied. In this case distribution of the reaction efficiency is not as strongly bimodal as in the case previously mentioned.

We have monitored the variation in the mean square radius

and the energy during the polymer folding as a function of time. They show somewhat different behavior. $\langle R^2 \rangle$ and $\langle R_g^2 \rangle$ start decaying only after an initial characteristic time delay. The total energy of polymer chain starts decaying immediately after the quench and continues to do so till it reaches the final stable minimum energy configuration. This is because initial decrease of energy does not require change in R_0 – it occurs by establishing favorable contacts.

4 Conclusion

To conclude, we have shown in this work that a bimodal distribution of excitation transfer efficiency and of reaction times emerge during folding and unfolding of model homopolymers in solution. The distribution looks surprisingly similar to the ones observed recently in the folding of real proteins by single molecule spectroscopy. The extent of bimodality is found to depend on the values of the Forster parameters (k_{rad} and R_F), k_{rn} and the value of the diffusion coefficient (that is, the viscosity). Thus, a study like the one performed here can be useful in designing FRET experiments *via* single molecule spectroscopy. The present study suggests several exciting future problems. Both for folding and unfolding, one can initiate the FRET process after a suitable time lag (τ) following the quench and can thus obtain a *two dimensional distribution* of $P(\Phi_F,\tau)$, like in NMR or ESR. FRET may also be able to differentiate between different collapsed states, like rod and toroid.[2,3] Simulations of this can be carried out by using a stiff polymer chain.[2,3] Simulation study by using more realistic models and also by incorporating the solvent molecules implicitly, may reveal more information. Further work in these directions is under progress. Finally, simulations of $P(\Phi_F)$ during folding of real proteins remain a challenging task.

Acknowledgement

It is pleasure to thank Prof. A. Yethiraj for the help and discussion. The financial support from CSIR, New Delhi, India and DST India is gratefully acknowledged. G. Srinivas thanks CSIR for a research fellowship.

References

1 Y. Zhou, C. K. Hall and M. Karplus, *Phys. Rev. Lett.*, 1996, **77**, 2822; Y. Zhou, M. Karplus, J. M. Wichert and C. K. Hall, *J. Chem. Phys.*, 1997, **107**, 10691.
2 (*a*) H. Noguchi and K. Yoshikawa, *J. Chem. Phys.*, 2000, **113**, 854; (*b*) H. Noguchi and K. Yoshikawa, *J. Chem. Phys.*, 1998, **109**, 5070.
3 D. Hu, J. Yu, K. Wong, B. Bagchi, P. Rossky and P. F. Barbara, *Nature*, 2000, **405**, 1030.
4 K. Yue and K. A. Dill, *Phys. Rev. E*, 1993, **48**, 2267; H. S. Chan and K. A. Dill, *Proc. Natl. Acad. Sci. USA*, 1990, **87**, 6368.
5 P. G. Wolynes, *Proc. Natl. Acad. Sci. USA*, 1997, **94**, 6170; J. D. Bryngelson and P. G. Wolynes, *J. Phys. Chem.*, 1989, **93**, 6902.
6 J. N. Onuchic, P. G. Wolynes, Z. Luthey-Schulten and N. D. Socci, *Proc. Natl. Acad. Sci. USA*, 1995, **92**, 3626.
7 D. K. Klimov and D. Thirumalai, *Phys. Rev. Lett.*, 1996, **76**, 4070; D. Thirumalai and S. A. Woodson, *Acc. Chem. Res.*, 1996, **29**, 433.
8 A. M. Gutin, V. Abkenvich and E. I. Shaknovich, *Phy. Rev. Lett.*, 1996, **77**, 5433.
9 A. A. Deniz, T. A. Laurence, G. S. Beligere, M. Dahan, A. B. Martin, D. S. Chemla, P. E. Dawson, P. G. Schultz and S. Weiss, *Proc. Natl. Acad. Sci. USA*, 2000, **97**, 5179; A. A. Deniz, M. Dahan, J. R. Grunwell, T. Ha, A. E. Faulhaber, D. S. Chemla, S. Weiss and P. G. Schultz, *Proc. Natl. Acad. Sci. USA*, 1999, **96**, 3670; S. Weiss, *Science*, 1999, **283**, 676.
10 D. S. Talaga, W. L. Lau, H. Roder, J. Tang, W. F. DeGrado and R. M. Hoschstrasser, *Proc. Natl. Acad. Sci. USA*, 1999, **97**, 13021.
11 M. I. Wallace, L. Ying, S. Balasubramanian and D. Klenermen, *J. Phys. Chem. B*, 2000, **104**, 11551; M. I. Wallace, L. Ying, S. Balasubramanian and D. Klenermen, *J. Phys. Chem. B*, 2000, **104**, 5171.
12 Th. Forster, *Ann. Phys. (Leipzig)*, 1948, **2**, 55; L. Stryer and R. P. Haugland, *Proc. Natl. Acad. Sci. USA*, 1967, **58**, 719.
13 L. Stryer and R. P. Haugland, *Proc. Natl. Acad. Sci. USA*, 1967, **58**, 719.
14 N. J. Turro, *Modern Molecular Photochemistry*, University Press, Menlo Park, CA, 1978.
15 (*a*) G. Srinivas, A. Yethiraj and B. Bagchi, *J. Phys. Chem. B*, 2001, **105**, 2475; (*b*) G. Srinivas and B. Bagchi, *Chem. Phys. Lett.*, 2000, **328**, 420.